DSP-BASED SUPPRESSION OF SPURIOUS EMISSIONS AT RX BAND IN CARRIER AGGREGATION FDD TRANSCEIVERS

Adnan Kiayani, Mahmoud Abdelaziz, Lauri Anttila, Vesa Lehtinen and Mikko Valkama

Department of Electronics and Communications Engineering,
Tampere University of Technology, FI-33101, Tampere, Finland.
contact email: mikko.e.valkama@tut.fi

ABSTRACT

In frequency division duplex transceivers employing non-contiguous carrier aggregation (CA) transmission, achieving sufficient isolation between transmit and receive chains using radio frequency filtering alone is increasingly difficult. Particularly challenging problem in this context is spurious intermodulation (IM) components due to nonlinear power amplifier (PA), which may easily overlap the receiver band. With realistic duplex filters, the residual spurious IM at RX band can be several dBs stronger than the thermal noise floor, leading to own receiver desensitization. In this paper, we carry out detailed signal modeling of spurious emissions due to wideband PAs at the third-order IM band. Stemming from this modeling, and using the known transmit data, we present an efficient nonlinear digital identification and cancellation technique to suppress the unwanted IM components at RX band. The proposed technique is verified with computer simulations, showing excellent calibration properties, hence relaxing filtering and duplexing distance requirements in spectrally-agile CA transceivers.

Index Terms— Cancellation, carrier aggregation, duplexer isolation, frequency division duplexing, intermodulation, LTE-Advanced, power amplifier, spurious emissions.

1. INTRODUCTION

In order to cope with the ever increasing demands of mobile users for multimedia and other broadband services, the 3rd Generation Partnership Project (3GPP) in its Release 10 Long Term Evolution-Advanced (LTE-A) standard has introduced Carrier Aggregation (CA) [1], which enables scalable bandwidth expansion beyond 20 MHz by aggregating two or more component carriers (CCs). Besides spectral efficiency and offering data rates of up to 1 Gbps in downlink and 500 Mbps in uplink, other key features of LTE-A include flexible bandwidths, low latency, multi-antenna transmission, and backward compatibility to Release 8/9 [2]. While CA is supported
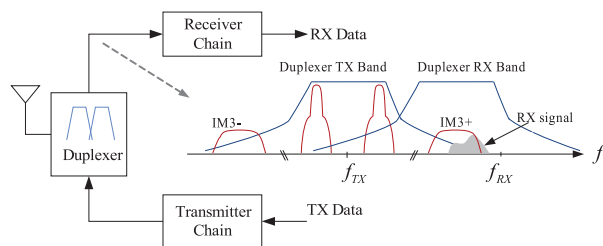
Fig. 1. Illustration of TX induced spurious IM3 emissions at RX band with non-contiguous TX carriers.

by both Frequency Division Duplex (FDD) and Time Division Duplex (TDD) modes of LTE-A, in this article we concentrate on the linearity challenges in CA FDD transceivers and suppression of spurious IM3 emissions at own receiver band.

In mobile radio transceivers operating in FDD mode, a duplexer filter is employed to facilitate simultaneous transmission and reception with a single antenna, while also providing isolation between the TX and RX chains. When emphasizing power efficiency and flexible spectrum use, strong intermodulation distortion (IM) products of the transmit signal, created by a nonlinear power amplifier (PA), result in spurious emissions that may appear in the RX band. This is illustrated in Fig. 1, where positive IM3 components lie at own RX band. Due to finite duplexer filter attenuation [4] and considerably narrow duplexing gaps in systems such as LTE-A, the remaining spurious emissions at the duplexer output at the RX band can potentially be of similar magnitude or even higher than the actual received signal. This can thus lead to own receiver desensitization. To demonstrate the own receiver desensitization phenomenon, consider LTE uplink band 25 [3] and assume intra-band CA with two carriers where duplexing gap is only 15 MHz. Assuming that the unwanted emissions at PA output, prior to duplexer, can in general be up to -30dBm/1MHz [3] (general spurious emission limit), and that duplexer isolation towards receiver at RX band is typically $50 - 60$ dB [4], the unwanted emission at RX input can thus be in the order of $-80 \cdots -90$dBm/1MHz. Compared to the effective thermal noise power with nominal 9dB UE RX noise figure, namely $-174 + 60 + 9 = -105$dBm/1MHz, this

is substantial interference and can completely block the receiver. Notice also that the general coexistence related emission limit of -50dBm/1MHz [3], applicable also at own RX band, is measured at antenna connector, and is thus totally insufficient to protect own RX.

Classical solutions to prevent own receiver desensitization in CA FDD transceivers are to either improve the duplexer TX filtering or to increase the duplex distance. Improving the duplexer filtering is, however, costly and may not be feasible for compact mobile transceivers supporting wider bandwidths and carrier frequencies with small duplexing distance. Alternative solutions using signal processing techniques to suppress the transmitter emissions in the receiver path are proposed in [7], [8] for FDD transceivers. These approaches create a replica of the emitted interference and then use it to suppress the interfering emissions at digital baseband. While [7] assumes known duplexer filter responses and memoryless PA model, the technique presented in [8] estimates the so called *transmitter leakage channel*, which is the collective response of duplexer filters and PA with memory. From the CA perspective, and especially non-contiguous CA transmission, where the total frequency span of the transmit signal can be in the order of 100 MHz or even beyond, these techniques are computationally challenging as they require digital processing of the whole transmission band and do not take the specific frequency-domain structure of the aggregated carriers into account. In contrast to this, we focus in this paper on lower-complexity solution particularly tailored to generic non-contiguous dual-carrier CA transmission scenario where unwanted IM3 spurious emissions desensitize the own receiver. Novel formulation for essential response identification and spurious emission regeneration and cancellation at digital baseband is developed, supporting unknown frequency-selective duplexer response and nonlinear PA with memory. The proposed solution can efficiently prevent own receiver desensitization, and can be seen as a novel extension of the authors' earlier work in [8].

Notations: scalar parameters are represented by lower case letters a and vectors/matrices in boldface letters **a**. We distinguish the vectors from matrices by a bold face letter with under-line **a**. The convolution operator is indicated by $\star$. Superscripts $(.)^T$ and $(.)^H$ denote the transpose and hermitian transpose, respectively, while $(.)^{-1}$ denotes matrix inverse.

2. SIGNAL MODELING FOR TX SPURIOUS EMISSIONS AT RX BAND IN CA FDD TRANSCEIVERS

In a CA FDD transceiver context with small duplexing distance and finite isolation duplexer filter, we consider a scenario where the IM3 band of the transmit signal overlaps with, and therefore creates significant interference, at the RX band. The relative strength of such interference depends in general on the duplexing distance, duplexer filter attenuation, transmit signal strength, and PA characteristics, and is elaborated in more details below.
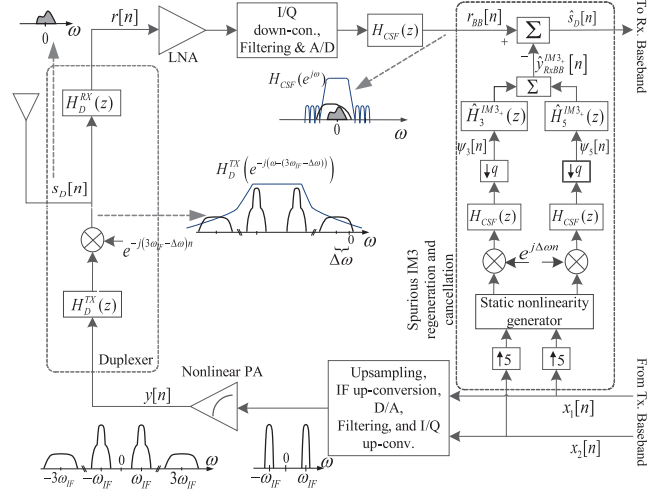

Fig. 2. Discrete-time baseband equivalent model and spectra of nonlinear transmit PA induced spurious emission at receiver band in an CA FDD transceiver. The proposed spurious IM3 emission regeneration and suppression unit operating at digital baseband is also shown, with 3rd and 5th order cancellation units.

In this paper, we assume a general non-contiguous dual-carrier CA FDD transceiver, for which the composite complex baseband/IF transmit signal, denoted by $x[n]$, is composed of two CCs that are separated by $2\omega_{IF}$. The IM3 distortion component, arising primarily due to the nonlinearity of PA and located at three times the IF frequency, may then lie at the RX band. For analysis and modeling purposes, the frequency separation between the center frequencies of the IM3 component and the desired RX signal is denoted by $\Delta\omega$. Fig. 2 shows the discrete-time baseband equivalent model of such scenario and the associated signal spectra, with finite isolation duplexing filters and nonlinear transmitter PA.

In the TX chain, the composite dual-carrier baseband signal is up-converted to the transmitter carrier frequency and the RF signal is then amplified by a PA for transmission. Practical PAs have inherently a nonlinear response and exhibit memory effects for wideband signals. Among numerous models that exist for PAs with memory, we use here the parallel Hammerstein model with polynomial nonlinearities to express the nonlinearity of PA with memory effects, as it has been shown in literature to have very good modeling capabilities for wideband PAs [6]. The baseband equivalent PA input and output are then expressed as

$$x[n] = x_1[n]e^{j\omega_{IF}n} + x_2[n]e^{-j\omega_{IF}n} \qquad (1)$$

$$y[n] = \sum_{\substack{p=1 \\ p\ odd}}^{P} f_p[n] \star \left(x[n]\,|x[n]|^{p-1} \right) \qquad (2)$$

where $x_1[n]$ and $x_2[n]$ denote the baseband component carrier waveforms and P denotes the polynomial order. Substituting (1) in (2), the baseband equivalent positive and negative IM3

components, located at $3\omega_{IF}$ and $-3\omega_{IF}$ respectively in the composite signal, read

$$y^{IM3+}[n] = f_3^{IM3+}[n] \star x_1^2[n]x_2^*[n] + 3f_5^{IM3+}[n]\star$$
$$x_1^2[n]x_2^*[n]\,|x_2[n]|^2 + 2f_5^{IM3+}[n] \star x_1^2[n]x_2^*[n]\,|x_1[n]|^2 \quad (3)$$

$$y^{IM3-}[n] = f_3^{IM3-}[n] \star x_1^*[n]x_2^2[n] + 3f_5^{IM3-}[n]\star$$
$$x_1^*[n]x_2^2[n]\,|x_1[n]|^2 + 2f_5^{IM3-}[n] \star x_1^*[n]x_2^2[n]\,|x_2[n]|^2 \quad (4)$$

where nonlinearity orders up to $P = 5$ are considered, and $f_3^{IM3\pm}[n]; f_5^{IM3\pm}[n]$ are the corresponding baseband equivalent filters modeling the PA's frequency-responses for 3rd and 5th order nonlinearities at positive and negative IM3 bands, respectively, defined as $f_3^{IM3\pm}[n] = h_{LPF}[n] \star \left(f_3[n]e^{\mp j3\omega_{IF}n}\right); f_5^{IM3\pm}[n] = h_{LPF}[n] \star \left(f_5[n]e^{\mp j3\omega_{IF}n}\right)$. For simplicity, we assume below that the positive IM3 term $y^{IM3+}[n]$ appears at the RX operating band and thus focus on its further modeling and cancellation.

The PA output signal then passes through the duplexer to the antenna. A duplexer is constructed with two band pass filters. In the transmitter path, the transmitter duplex filter tries to attenuate the unwanted emissions outside the transmit band, especially the transmitter noise from PA present at the receiver frequency band. The receiver duplex filter then attenuates the transmitter passband signal leaking into the receiver chain. With finite attenuation of duplexing filters, transmitter spurious emissions are not completely suppressed and thus cause self-interference at RX band.

At the receiver input, the baseband equivalent positive IM3 component leaking into the RX band after passing through the cascade of transmitter and receiver duplexer filters can be mathematically expressed as

$$y_{leak}^{IM3+}[n] = h_D[n] \star \left(y^{IM3+}[n]e^{j\Delta\omega n}\right). \quad (5)$$

The cumulative duplexer filter response from TX-RX leakage perspective, denoted by $h_D[n]$ in the above equation, is defined as

$$h_D[n] = h_D^{RX}[n] \star \left(h_D^{TX}[n]e^{-j(3\omega_{IF}-\Delta\omega)n}\right) \quad (6)$$

where $h_D^{TX}[n]; h_D^{RX}[n]$ represent the baseband equivalent lowpass models of the bandpass TX and RX duplexer filters, respectively. In addition to the transmitter spurious emissions, the desired received signal, denoted by $s_D[n]$, and the thermal noise, denoted by $w[n]$, are also present. Thus, the baseband equivalent composite received signal at the receiver input is

$$r[n] = s_D[n] + y_{leak}^{IM3+}[n] + w[n]. \quad (7)$$

This signal is subsequently down-converted from RF to baseband by the receiver local oscillator (LO), followed by the channel selection filtering (CSF), denoted here by $h_{CSF}[n]$. The baseband signal at the CSF output is then given by

$$r_{BB}[n] = h_{CSF}[n] \star r[n] = s_D[n] + y_{RxBB}^{IM3+}[n] + w_{BB}[n] \quad (8)$$

where $y_{RxBB}^{IM3+}[n] \triangleq h_{CSF}[n] \star y_{leak}^{IM3+}[n]$ denotes the unwanted spurious IM3 in the RX baseband and $w_{BB}[n] = h_{CSF} \star w[n]$ is the filtered inband noise.

As discussed already earlier, the transmitter duplexer filter may not have sufficient attenuation to push the transmitter spurious emissions below the thermal noise floor in the transceivers of next generation wireless systems such as LTE-A. Hence, in the following, we develop an efficient digital technique for dynamically regenerating the spurious IM3 component at the RX band and then subsequently suppressing it inside the FDD transceiver.

3. PROPOSED SPURIOUS IM3 REGENERATION AND CANCELLATION

Stemming from previous modeling, we now address the regeneration of positive spurious IM3 emission and its cancellation. The proposed framework appropriately estimates the *effective IM3 channel*, a cascade of unknown duplexer filter responses and the unknown nonlinear PA with memory at positive IM3 band. The estimated effective IM3 channel filters together with the known transmit data are used to create a replica of transmitter spurious emission at IM3 band.

3.1. Linear-in-Parameters Model of Spurious IM3

We first write the spurious IM3 emission term $y_{RxBB}^{IM3+}[n]$ in (8) in its equivalent form as

$$y_{RxBB}^{IM3+}[n] = h_{CSF}[n] \star y_{leak}^{IM3+}[n]$$
$$= h_3^{IM3}[n] \star \psi_3[n] + h_5^{IM3}[n] \star \psi_5[n] \quad (9)$$

where $h_p^{IM3}[n], p = 3, 5$ denote the effective IM3 channels, with subscript p representing the 3rd and 5th order PA nonlinearity filters, defined as

$$h_3^{IM3+}[n] \triangleq e^{j\Delta\omega n}\left(h_D[n] \star f_3^{IM3+}[n]\right)$$
$$h_5^{IM3+}[n] \triangleq e^{j\Delta\omega n}\left(h_D[n] \star f_5^{IM3+}[n]\right), \quad (10)$$

and the known component carrier baseband waveforms, duplexing distance, and CSF filter response are combined together to form the *modified filtered basis functions*, defined below as

$$\psi_3[n] \triangleq h_{CSF}[n] \star \left(x_1^2[n]x_2^*[n]\right)e^{j\Delta\omega n}$$
$$\psi_5[n] \triangleq h_{CSF}[n] \star \left(\begin{matrix} 3x_1^2[n]x_2^*[n]\,|x_2[n]|^2 + \\ 2x_1^2[n]x_2^*[n]\,|x_1[n]|^2 \end{matrix}\right)e^{j\Delta\omega n}. \quad (11)$$

With the linear-in-parameters model at last row of (9), the proposed IM3 regeneration and cancellation algorithm requires only estimation of the coefficients of effective IM3 channel filters $h_p^{IM3}[n]$, as other parameters such as the duplexing distance, digital transmit data, and the CSF filter response are known inside the transceiver. The principal regeneration and cancellation structure, stemming from above formulation, is also illustrated in Fig.2. Notice that the sample rate in the

modified filtered basis functions generation is only relative to bandwidths of the individual component carriers instead of the total aggregate bandwidth as in [8]. Furthermore, the cancellation is performed at the sample rate of the receiver chain.

3.2. LS Estimation of Effective IM3 Channel Filters

For parameter estimation of effective IM3 channels, we switch to vector-matrix notations and consider $N-$samples of each CC. By modeling both nonlinearity orders with N_h-taps, the effective IM3 channel filter vector is then of dimension $2N_h \times 1$. The spurious IM3 term in (9) then takes the form

$$\underline{\mathbf{y}}_{RxBB}^{IM3_+} = \mathbf{\Psi}_3 \underline{\mathbf{h}}_3^{IM3_+} + \mathbf{\Psi}_5 \underline{\mathbf{h}}_5^{IM3_+} = \begin{bmatrix} \mathbf{\Psi}_3 & \mathbf{\Psi}_5 \end{bmatrix} \begin{bmatrix} \underline{\mathbf{h}}_3^{IM3_+} \\ \underline{\mathbf{h}}_5^{IM3_+} \end{bmatrix}$$
$$= \mathbf{\Psi}\underline{\mathbf{h}}^{IM3_+}$$
(12)

where $\mathbf{\Psi}_p, p = 3, 5$, in $\mathbf{\Psi}$ is a matrix of dimension $(N + N_h - 1) \times N_h$, defined as

$$\mathbf{\Psi}_p = \begin{bmatrix} \psi_p[0] & 0 & \cdots & 0 \\ \psi_p[1] & \psi_p[0] & \cdots & 0 \\ \vdots & 0 & \cdots & 0 \\ \psi_p[N-1] & \vdots & \ddots & \vdots \\ 0 & \psi_p[N-1] & \cdots & \psi_p[N-N_h] \\ 0 & 0 & \cdots & \psi_p[N-N_h+1] \\ \vdots & \vdots & \ddots & \vdots \\ 0 & 0 & \cdots & \psi_p[N-1] \end{bmatrix}.$$
(13)

The total baseband received signal then becomes

$$\underline{\mathbf{r}}_{BB} = \underline{\mathbf{s}}_D + \mathbf{\Psi}\underline{\mathbf{h}}^{IM3_+} + \underline{\mathbf{w}}_{BB}.$$
(14)

Now, to estimate the effective IM3 channel parameters, we re-write (14) as

$$\underline{\mathbf{r}}_{BB} = \mathbf{\Psi}\underline{\mathbf{h}}^{IM3_+} + \underline{\mathbf{w}}_1$$
(15)

where $\underline{\mathbf{w}}_1 = \underline{\mathbf{s}}_D + \underline{\mathbf{w}}_{BB}$. The LS parameter estimate of $\underline{\mathbf{h}}^{IM3_+}$ is then given directly by [9]

$$\hat{\underline{\mathbf{h}}}^{IM3_+} = \left(\mathbf{\Psi}^H \mathbf{\Psi}\right)^{-1} \mathbf{\Psi}^H \underline{\mathbf{r}}_{BB}.$$
(16)

Finally, the estimates of effective IM3 channel filters are then used in the spurious IM3 emission regeneration and cancellation, as shown in Fig. 2.

4. SIMULATION RESULTS

In this section, we demonstrate the effectiveness of the proposed estimation and cancellation algorithm in a dual-carrier CA FDD transceiver. The simulation chain is set up according to Fig. 2, where the baseband transmit signal is a dual-carrier LTE-A uplink SC-FDMA signal. Each CC is allocated 50 resource blocks (RBs) that are separated by 50 MHz, and subcarrier modulation is QPSK. In the transmitter chain, PA with memory is modeled as a 5th order Wiener system with a linear filter, whose impulse response is $\underline{\mathbf{h}}_{wiener} = \begin{bmatrix} 1 & 0.2 & 0.34 & 0.068 & 0.0136 & 0.0027 & 0.0005 \end{bmatrix}^T$, and the memoryless nonlinearity coefficients are calculated from PA gain, IIP3, and $1-$dB compression point, which are 20 dB, 17 dBm, and 26 dBm, respectively. The mismatch between actual and assumed PA model is to mimic a practical scenario. The duplexer filter is modeled to have an average attenuation of 50 dB at the IM3 band, containing also frequency selectivity. We assume that the frequency separation between the center frequencies of positive IM3 component and the desired RX signal is $\Delta f = 2$ MHz. The RX signal is an LTE-A downlink OFDM(A) signal with 50 RBs, QPSK subcarrier modulation. The reference thermal noise power level at receiver input is assumed to be -104 dBm per 10 MHz bandwidth, RX noise figure (NF) is 4.5 dB, and the reference sensitivity level is -93.5 dBm. For the estimation and cancellation processing, we use sampling frequency $f_s = 30.72$ MHz which is only 2 times the nominal baseband sampling frequency of the individual TX and RX carriers. A block of 50 k samples of filtered baseband received signal $\underline{\mathbf{r}}_{BB}$ and the modified filtered basis function $\mathbf{\Psi}$ are used for estimating the effective IM3 channel parameters, which is modeled with $16-$taps ($N_h = 8$). The estimated filter parameters are used to regenerate the interfering IM3 component which is then subtracted from the composite baseband received signal.

In Fig. 3, we plot the essential power spectra before and after the proposed digital cancellation. The actual received signal and noise, both of which are ON during the parameter estimation, are also shown in the figure. It can be observed that with small duplexing distance and finite duplexer isolation, the strong spurious IM3 completely masks the received signal and corrupts the reception heavily. However, the proposed technique is able to push this undesired self-interference below the thermal noise floor in the receiver band when a proper set of nonlinear filters is used. It is interesting to note that considering only the third order PA nonlinearity already gives substantial improvement in performance but there is still some residual interference left in the RX signal band. Whereas, taking into account also the fifth order PA nonlinearity at IM3 band effectively mitigates the total interference.

To further quantify the performance, the desired received signal-to-interference plus noise ratio (SINR) is evaluated against different TX power levels. The SINR curves with different RX signal levels are depicted in Fig. 4. The results indicate that for transmit power levels less than 12 dB, the power of interfering spurious IM3 at the receiver band is negligibly small and does not deteriorate SINR. However, higher transmission levels generate more powerful spurious IM3 component which consequently degrades the receiver SINR. Nevertheless, the proposed technique is able to reduce the interference and to enhance SINR. With practical 23 dBm

TX power, the difference between interference free SNR and SINR with interference is about 30 dB. This difference reduces to less than 1 dB when the cancellation technique is employed. Furthermore, note that for TX powers > 21 dB, both 3rd and 5th order PA nonlinearities should be considered in the estimation and regeneration to effectively remove the interference. The simulation example further demonstrates that the proposed technique is able to efficiently estimate the IM3 leakage filters even in the presence of strong RX signal. Thus, the effectiveness of proposed solution is evident.

5. CONCLUSION

This paper addressed the problem of spurious IM3 emissions at receiver band in CA FDD transceivers. More specifically, the combination of small duplex gaps, practical PAs exhibiting memory effects, and practical duplexers with limited isolation may result in significant spurious emissions falling at the RX band and can easily lead to own receiver desensitization. A nonlinear estimation and regeneration procedure was proposed, where first the unknown duplexer response and unknown nonlinear PA with memory response at IM3 band are estimated, and then used to reproduce and suppress the unwanted spurious IM3 components at own receiver digital baseband. This enables efficient mitigation of spurious IM3 emissions hence relaxing duplex distance and duplexer filtering requirements and thereby increasing the flexibility of the transceiver. The proposed technique was evaluated with computer simulations showing that spurious emissions can be effectively suppressed below the noise floor. Future work will focus on a prototype implementation and RF measurements to demonstrate the suppression properties of the proposed algorithms with real RF duplexers and PAs.

REFERENCES

[1] M. Iwamura *et al.*, "Carrier aggregation framework in 3GPP LTE-advanced", *IEEE Commun. Mag.*, vol. 48, no. 8, pp. 60-67, August 2010.

[2] S. Sesia, I. Toufik, and M. Baker, *LTE-The UMTS Long Term Evolution, From Theory to Practice*, Chichester, West Sussex, John Wiley & Sons Ltd., 2008.

[3] 3GPP "TS 36.101: Evolved Universal Terrestrial Radio Access (E-UTRA);User Equipment (UE) radio transmission and reception", Release 11, Nov. 2012.

[4] Ericsson and ST-Ericsson, *R4-126964, REFSENS with one UL carrier for NC intra-band CA*.

[5] "Evolved Universal Terrestrial Radio Access (E-UTRA); Radio Frequency (RF) system scenarios", 3GPP Tech. Report v. 10.2.0, Release 10, TR 36.942, May 2011.

[6] M. Isaksson, D. Wisell, and D. Rönnow, "A comparative analysis of behavioral models for RF power amplifiers," *IEEE Trans. Microw. Theory Tech.,* vol. 54, no. 1, pp. 348359, Jan. 2006.

[7] M. Omer *et al.*, "A compensation scheme to allow full duplex operation in the presence of highly nonlinear microwave components for 4G systems," in Proc. *IEEE MTT-S Int. Microwave Symp. Dig.*, June 2011.

[8] A. Kiayani, L. Anttila, and M. Valkama, "Digital suppression of power amplifier spurious emissions at receiver band in FDD transceivers, "*IEEE Signal Processing Letters,* vol. 21, no. 1, pp. 69-73, Jan. 2014.

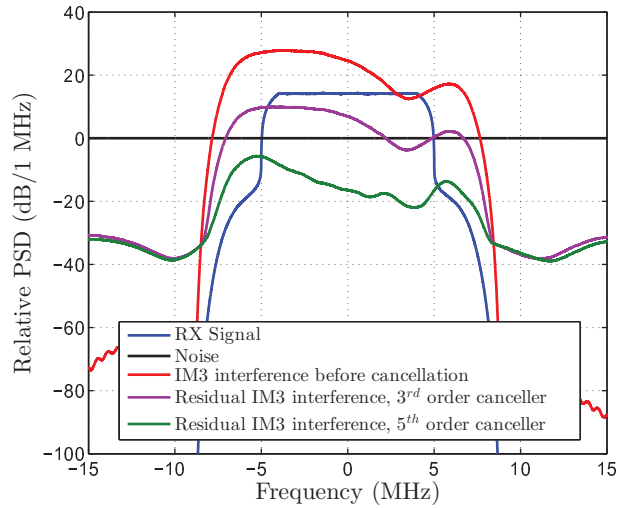[9] S. Haykin, *Adaptive Filter Theory*, 4th ed. Upper Saddle River, NJ: Prentice-Hall, 2002.

Fig. 3. Spurious IM3 emission at RX band before and after cancellation with 23 dBm TX Power and 5th-order Wiener PA. The RX signal is 10 dB above the REFSENS level. PSDs are normalized to the noise power.

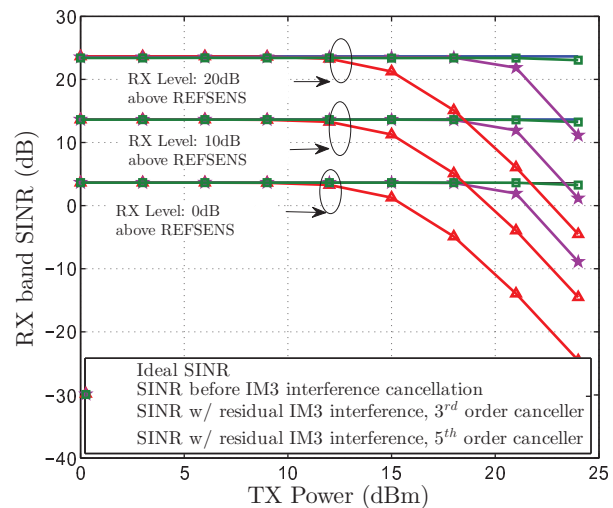**Fig. 4**. Comparison of average SINR vs. TX power before and after cancellation with different RX signal strengths.